

Preparation, Characterization, and Structural Systematics of Diphosphane and Diarsane Complexes of Indium(III) Halides

Fei Cheng, Sarah I. Friend, Andrew L. Hector, William Levason,* Gillian Reid, Michael Webster, and Wenjian Zhang

School of Chemistry, University of Southampton, Southampton, United Kingdom SO17 1BJ

Received June 13, 2008

The ligands $\sigma\text{-C}_6\text{H}_4(\text{PMe}_2)_2$ and $\sigma\text{-C}_6\text{H}_4(\text{AsMe}_2)_2$ (L–L) react with anhydrous InX_3 (X = Cl, Br, or I) in a 2:1 InX_3 /ligand ratio to form $[\text{InX}_2(\text{L}-\text{L})][\text{InX}_4]$ containing distorted tetrahedral cations, established by X-ray crystal structures for L–L = $\sigma\text{-C}_6\text{H}_4(\text{PMe}_2)_2$ (X = Br or I) and $\sigma\text{-C}_6\text{H}_4(\text{AsMe}_2)_2$ (X = I). IR, Raman, and multinuclear NMR (^1H , ^{31}P , ^{115}In) spectroscopy show that these are the only species present in solution in chlorocarbons and in the bulk solids. The products from reactions in a 1:1 or 1:2 molar ratio are more diverse and include the halide-bridged dimers $[\text{In}_2\text{Cl}_6\{\sigma\text{-C}_6\text{H}_4(\text{PMe}_2)_2\}_2]$ and $[\text{In}_2\text{X}_6\{\sigma\text{-C}_6\text{H}_4(\text{AsMe}_2)_2\}_2]$ (X = Cl or Br) and the distorted octahedral cation *trans*- $[\text{InBr}_2\{\sigma\text{-C}_6\text{H}_4(\text{PMe}_2)_2\}_2][\text{InBr}_4]$. The neutral complexes partially rearrange in chlorocarbon solution, with multinuclear NMR spectroscopy revealing $[\text{InX}_4]^-$ among other species. The iodo complexes *trans*- $[\text{InI}_2(\text{L}-\text{L})_2][\text{InI}_4(\text{L}-\text{L})]$ contain rare examples of six-coordinate anions, as authenticated by an X-ray crystal structure for L–L = $\sigma\text{-C}_6\text{H}_4(\text{PMe}_2)_2$. Two species of formula $[\text{In}_2\text{Cl}_5(\text{L}-\text{L})_n][\text{InCl}_4]_n$ (L–L = $\sigma\text{-C}_6\text{H}_4(\text{PMe}_2)_2$ and $\sigma\text{-C}_6\text{H}_4(\text{AsMe}_2)_2$) were identified crystallographically and contain polymeric cations with six-coordinate indium centers bonded to one chelating L–L and a terminal chlorine, linked by alternating single and double chlorine bridges into chains. The complicated chemistry of InX_3 with these two rigid chelates is contrasted with that of the flexible diphosphane $\text{Et}_2\text{P}(\text{CH}_2)_2\text{PEt}_2$, which forms $[\text{In}_2\text{Cl}_6\{\text{Et}_2\text{P}(\text{CH}_2)_2\text{PEt}_2\}_2]$, and with more sterically demanding $\sigma\text{-C}_6\text{H}_4(\text{PPh}_2)_2$ (Sigl et al. *Eur. J. Inorg. Chem.* **1998**, 203–210). The results also contrasted with those found for GaX_3 with the same ligands (Cheng et al. *Inorg. Chem.* **2007**, 46, 7215–7223).

Introduction

The heavier p-block metals have a rich coordination chemistry, which only in recent years has been explored in any significant detail.^{1,2} Compared with the familiar d-block chemistry, that of the p-block is more restricted in the range of accessible oxidation states and lacks a simple bonding model corresponding to ligand field theory, which can rationalize and predict many of the detailed trends in the chemistry. The factors which determine stoichiometries and structures are often unclear, and in relatively few systems has the “fine tuning” of the metal properties by ligand design been explored in detail. As pointed out by Downs,³ in group

13, there are many similarities in the chemistries of the elements, but even within the heavier metallic elements, the properties vary in a highly irregular fashion.

Applications of indium lie mainly in the electronics industries in III–V semiconductors such as InP and InSb,⁴ although there is growing use of indium reagents in organic synthesis,⁵ and the radio-nuclides ^{111}In and $^{113\text{m}}\text{In}$ as medical imaging agents.⁶

Tertiary phosphanes mostly form trigonal bipyramidal complexes with indium(III) halides $[\text{InX}_3(\text{PR}_3)_2]$ (X = Cl, Br or I),⁷ although a limited number of pseudo-tetrahedral

* Author to whom correspondence should be addressed. E-mail: wx1@soton.ac.uk.

- (1) Greenwood, N. N.; Earnshaw, A. *Chemistry of the Elements*, 2nd ed.; Butterworth-Heinemann: Oxford, U.K., 1997.
- (2) McCleverty, J. A.; Meyer, T. J. *Comprehensive Coordination Chemistry II*; Elsevier: Oxford, U.K., 2004; Vol. 3.
- (3) Downs, A. J. *Chemistry of Aluminium, Gallium, Indium and Thallium*; Blackie: London, 1993.

- (4) (a) O'Brien, P.; Pickett, N. L. In *Comprehensive Coordination Chemistry II*; McCleverty, J. A., Meyer, T. J., Eds.; Elsevier: Oxford, U.K., 2004; Vol. 9, pp 1005–1063. (b) Grant, I. R. In *Chemistry of Aluminium, Gallium, Indium and Thallium*; Downs, A. J., Ed.; Blackie: London, 1993, Chapter 5.
- (5) Starowieyski, K. B. In *Chemistry of Aluminium, Gallium, Indium and Thallium*; Downs, A. J., Ed.; Blackie: London, 1993, Chapter 6.
- (6) Anderson, C. J.; Welch, M. J. *Chem. Rev.* **1999**, 99, 2219–2234.
- (7) Norman, N. C.; Pickett, N. L. *Coord. Chem. Rev.* **1995**, 145, 27–54.

[InX₃(PR₃)] have also been characterized.^{8,9} Diphosphane complexes include a few structurally characterized examples of Ph₂P(CH₂)₂PPh₂ κ^1 - or μ_2 -coordinated to InI₃,^{7,9,10} but the only systematic study¹¹ is with the ligand *o*-C₆H₄(PPh₂)₂, which formed *trans*-[InCl₂{*o*-C₆H₄(PPh₂)₂}]₂[InCl₄], [InX₃{*o*-C₆H₄(PPh₂)₂}], and [InX₂{*o*-C₆H₄(PPh₂)₂}]₂[InX₄] (X = Br or I). Very little is known about diarsane complexes.¹²

Here, we report systematic studies of the reactions of indium(III) halides with the ligands *o*-C₆H₄(PMe₂)₂, *o*-C₆H₄(AsMe₂)₂, *o*-C₆H₄(PPh₂)₂, and Et₂P(CH₂)₂PEt₂, to explore the effects of the ligand donor and architecture upon the stoichiometries and structures produced. Direct comparisons are drawn with results from our recent work on gallium(III) complexes of these ligands.¹³

Experimental Section

Anhydrous indium halides were obtained from Aldrich and used as received. Ligands were obtained from Aldrich (Et₂P(CH₂)₂PEt₂) or were made by literature methods: *o*-C₆H₄(PPh₂)₂, *o*-C₆H₄(PMe₂)₂, and *o*-C₆H₄(AsMe₂)₂.^{14–16} All reactions were conducted using Schlenk, vacuum line, and glovebox techniques and under a dry dinitrogen atmosphere. IR spectra were recorded from Nujol mulls on a Perkin-Elmer PE 983G spectrometer, and Raman spectra were recorded using a Perkin-Elmer FT Raman 2000R with a Nd:YAG laser. ¹H NMR spectra were recorded from solutions in CDCl₃ or CD₂Cl₂ on a Bruker AV300, and ¹¹⁵In and ³¹P{¹H} NMR spectra were recorded on a Bruker DPX400 and referenced to [In(H₂O)₆]³⁺ in water at pH = 1 and 85% H₃PO₄, respectively. Microanalytical results were from the University of Strathclyde or Medac Ltd.

[InCl₂{*o*-C₆H₄(PMe₂)₂}]₂[InCl₄] (1). InCl₃ (0.27 g, 1.2 mmol) was dissolved in toluene (10 mL), *o*-C₆H₄(PMe₂)₂ (0.12 g, 0.6 mmol) added, and the mixture heated and stirred at 80 °C for 2 h. It was cooled to room temperature, and the white precipitate was filtered off and dried in vacuo. Yield: 0.36 g, 94%. Anal. calcd for C₁₀H₁₆Cl₆In₂P₂ (640.5): C, 18.8; H, 2.5. Found: C, 19.2; H, 2.4. ¹H NMR (300 MHz, CD₂Cl₂, 295 K): 1.90 (t, [6H], ²J + ⁵J = 6 Hz, CH₃), 7.70–7.90 (m, [2H], C₆H₄). ³¹P{¹H} NMR (CH₂Cl₂/CDCl₃, 295 K): –36.5 (s, br), unchanged on cooling. ¹¹⁵In NMR (CH₂Cl₂/CDCl₃, 295 K): +456. IR (cm⁻¹, Nujol): 339(m), 321(m), 297(w). Raman (cm⁻¹): 342(m), 322(vs), 297(m).

[InBr₂{*o*-C₆H₄(PMe₂)₂}]₂[InBr₄] (2). This was prepared similarly to the chloride complex, from *o*-C₆H₄(PMe₂)₂ (0.06 g, 0.3 mmol) and InBr₃ (0.20 g, 0.6 mmol). White solid. Yield: 0.243 g, 66%. Anal. calcd for C₁₀H₁₆Br₆In₂P₂·1/4C₇H₈ (930.3): C, 15.1; H, 2.0. Found: C, 15.0; H, 2.1. ¹H NMR (300 MHz, CD₂Cl₂, 295 K): 1.94 (t, [6H], ²J + ⁵J = 4 Hz, CH₃), 7.83–7.96 (m, [2H], C₆H₄), and

weak toluene resonances. ³¹P{¹H} NMR (CH₂Cl₂/CDCl₃, 295 K): –38.2(s), unchanged on cooling. ¹¹⁵In NMR (CH₂Cl₂/CDCl₃, 295 K): +178. IR (cm⁻¹, Nujol): 257(w), 228(m), 224(w). Raman (cm⁻¹): 264(w), 234(m), 221(m), 198(vs).

[InI₂{*o*-C₆H₄(PMe₂)₂}]₂[InI₄] (3). This was prepared similarly to the chloride analogue from *o*-C₆H₄(PMe₂)₂ (0.06 g, 0.3 mmol) and InI₃ (0.30 g, 0.6 mmol). White solid. Yield: 0.243 g, 68%. Anal. calcd for C₁₀H₁₆I₆In₂P₂ (1189.3): C, 10.1; H, 1.3. Found: C, 10.3; H, 1.4. ¹H NMR (300 MHz, CD₂Cl₂, 295 K): 1.99 (t, [6H], ²J + ⁵J = 4 Hz, CH₃), 7.90–8.00 (m, [2H], C₆H₄). ³¹P{¹H} NMR (CH₂Cl₂/CDCl₃, 295 K): –42.2(s). ¹¹⁵In NMR (CH₂Cl₂/CDCl₃, 295 K): –565. IR (cm⁻¹, Nujol): 190(sh), 185(m). Raman (cm⁻¹): 192(vs).

[InBr₂{*o*-C₆H₄(PMe₂)₂}]₂[InBr₄] (4). Prepared using the above method with *o*-C₆H₄(PMe₂)₂ (0.12 g, 0.6 mmol) and InBr₃ (0.21 g, 0.6 mmol). White solid. Yield: 0.29 g, 88%. Anal. calcd for C₂₀H₃₂Br₆In₂P₄·1/4C₇H₈ (1128.5): C, 24.5; H, 3.2. Found: C, 25.1; H, 3.2. ¹H NMR (300 MHz, CD₂Cl₂, 295 K): 1.83 (s, [6H], CH₃), 7.68–7.91 (m, [2H], C₆H₄), and weak toluene resonances. ³¹P{¹H} NMR (CH₂Cl₂/CDCl₃, 295 K): –44.9(s). ¹¹⁵In NMR (CH₂Cl₂/CDCl₃, 295 K): +182. IR (cm⁻¹, Nujol): 240(sh), 233(m). Raman (cm⁻¹): 264(w), 236(m), 196(vs).

[InI₂{*o*-C₆H₄(PMe₂)₂}]₂ (5). A solution of *o*-C₆H₄(PMe₂)₂ (0.16 g, 0.8 mmol) in toluene (15 mL) was added to InCl₃ (0.18 g, 0.8 mmol). The solution was heated at 80 °C for 2 h, then cooled to room temperature. The resulting white precipitate was separated by filtration, then dried in vacuo. Yield: 0.29 g, 44%. Anal. calcd for C₂₀H₃₂Cl₆In₂P₄ (838.8): C, 28.6; H, 3.9. Found: C, 28.6; H, 3.4. ¹H NMR (300 MHz, CD₂Cl₂, 295 K): 1.83 (d, [6H], ²J = 11 Hz, CH₃), 7.71–7.91 (m, [2H], C₆H₄). ³¹P{¹H} NMR (CH₂Cl₂/CDCl₃, 295 K): –43.6(br); (248 K): –42.8, –44.2. ¹¹⁵In NMR (CH₂Cl₂/CDCl₃, 295 K): +442. IR (cm⁻¹, Nujol): 334(m), 282(m), 263(s). Raman (cm⁻¹): 335(m), 290(s), 280(vs), 260(sh).

[InI₂{*o*-C₆H₄(PMe₂)₂}]₂[InI₄{*o*-C₆H₄(PMe₂)₂}] (6). This was prepared using the method for the preceding complex with *o*-C₆H₄(PMe₂)₂ (0.10 g, 0.5 mmol) and InI₃ (0.25 g, 0.5 mmol). White solid. Yield: 0.349 g, 44%. Anal. calcd for C₃₀H₄₈I₆In₂P₆ (1585.6): C, 22.7; H, 3.1. Found: C, 23.3; H, 3.0. ¹H NMR (300 MHz, CD₂Cl₂, 295 K): 1.70 (br, s, [6H], CH₃), 7.65–7.79 (m, [2H], C₆H₄); (180 K): 1.64(s), 1.87(s), 7.71–7.86(m). ³¹P{¹H} NMR (CH₂Cl₂/CDCl₃, 295 K): –52.7(br); (273 K): –46.8, –55.0. ¹¹⁵In NMR (CH₂Cl₂/CDCl₃, 295 K): –564.

[InI₂{*o*-C₆H₄(AsMe₂)₂}]₂ (7). A solution of *o*-C₆H₄(AsMe₂)₂ (0.28 g, 0.9 mmol) in toluene (15 mL) was added to InCl₃ (0.10 g, 0.45 mmol) and the mixture heated at 80 °C for 2 h. The white product was isolated by cooling the solution to ambient temperatures and filtering off and drying in vacuo. Yield: 0.25 g, 55%. Anal. calcd for C₂₀H₃₂As₄Cl₆In₂ (1014.5): C, 23.7; H, 3.2. Found: C, 23.7; H, 3.3. ¹H NMR (400 MHz, CD₂Cl₂, 295 K): 1.75 (s, [6H], CH₃), 7.70–7.86 (m, [2H], C₆H₄); (213 K): 1.72 (s), 1.73 (s), 7.60–7.80 (m). ¹¹⁵In NMR (CH₂Cl₂/CDCl₃, 295 K): +451. IR (cm⁻¹, Nujol): 321(m), 277(m). Raman (cm⁻¹): 321(m), 277(s).

[InBr₂{*o*-C₆H₄(AsMe₂)₂}]₂ (8). This complex was prepared as above from *o*-C₆H₄(AsMe₂)₂ (0.17 g, 0.6 mmol) and InBr₃ (0.21 g, 0.6 mmol). White powder. Yield: 0.33 g, 86%. Anal. calcd for C₂₀H₃₂As₄Br₆In₂ (1281.2): C, 18.75; H, 2.52. Found: C, 18.7; H, 2.3. ¹H NMR (300 MHz, CD₂Cl₂, 295 K): 1.73 (s, [6H], CH₃), 7.60–7.80 (m, [2H], C₆H₄); (190 K): 1.75 (s), 7.70 (m). ¹¹⁵In NMR (CH₂Cl₂/CDCl₃, 295 K): +189. IR (cm⁻¹, Nujol): 222(m), 218(m). Raman (cm⁻¹): 237(m), 229(m).

[InI₂{*o*-C₆H₄(AsMe₂)₂}]₂[InI₄{*o*-C₆H₄(AsMe₂)₂}] (9). Prepared as above with *o*-C₆H₄(AsMe₂)₂ (0.22 g, 0.45 mmol) and InI₃ (0.13 g, 0.26 mmol). Cream solid. Yield: 0.26 g, 72%. Anal. calcd for

- (8) (a) Baker, L.-J.; Kloof, L. A.; Rickard, C. E. F.; Taylor, M. J. *J. Organomet. Chem.* **1997**, 545–546, 249–255. (b) Brown, M. A.; Tuck, D. G.; Wells, E. J. *Can. J. Chem.* **1996**, 74, 1535–1549. (c) Godfrey, S. M.; Kelly, K. J.; Kramkowski, P.; McAuliffe, C. A.; Pritchard, R. G. *Chem. Commun.* **1997**, 1001–1002.
- (9) Sigl, M.; Schier, A.; Schmidbaur, H. *Z. Naturforsch., B: Chem. Sci.* **1999**, 54, 21–25.
- (10) Degan, I. A.; Alcock, N. W.; Roe, S. M.; Wallbridge, M. G. H. *Acta Crystallogr., Sect. C* **1992**, C48, 995–999.
- (11) Sigl, M.; Schier, A.; Schmidbaur, H. *Eur. J. Inorg. Chem.* **1998**, 203–210.
- (12) Nyholm, R. S.; Ulm, K. *J. Chem. Soc.* **1965**, 4199–4203.
- (13) Cheng, F.; Hector, A. L.; Levason, W.; Reid, G.; Webster, M.; Zhang, W. *Inorg. Chem.* **2007**, 46, 7215–7223.
- (14) Kyba, E. P.; Liu, S. T.; Harris, R. L. *Organometallics* **1983**, 2, 1877–1879.
- (15) Feltham, R. D.; Nyholm, R. S.; Kasenally, A. J. *Organomet. Chem.* **1967**, 7, 285–288.
- (16) McFarlane, H. C. E.; McFarlane, W. *Polyhedron* **1983**, 2, 303–304.

$C_{30}H_{48}As_6In_2I_6$ (1585.6): C, 19.5; H, 2.6. Found: C, 18.7; H, 2.3. 1H NMR (300 MHz, CD_2Cl_2 , 295 K): 1.61 (s, [6H], CH_3), 7.66–7.80 (m, [2H], C_6H_4); (243 K): 1.57 (s, CH_3), 1.71 (s, CH_3), 7.66–7.80 (m, C_6H_4). ^{115}In NMR ($CH_2Cl_2/CDCl_3$, 295 K): –450 (vbr).

[InCl₂{*o*-C₆H₄(AsMe₂)₂}]₂[InCl₄] (10). *o*-C₆H₄(AsMe₂)₂ (0.120 g, 0.42 mmol) in toluene (2 mL) was added to a suspension of InCl₃ (0.186 g, 0.84 mmol) in toluene (5 mL), and the mixture was heated and stirred at 80 °C for 3 h. It was cooled to room temperature and the white precipitate filtered off and dried in vacuo. Yield: 93%. Anal. calcd for C₁₀H₁₆As₂Cl₆In₂ (728.4): C, 16.5; H, 2.2. Found: C, 18.0; H, 3.0 (this complex consistently gave poor microanalytical data, but no impurities or contained solvent was detected spectroscopically). 1H NMR (300 MHz, CD_2Cl_2 , 295K): 1.79 (s, [6H], CH_3), 7.6–7.7 (m, [2H], C_6H_4). ^{115}In NMR ($CH_2Cl_2/CDCl_3$, 295 K): –400 (vbr, W1/2, ~8000 Hz). IR (cm^{-1} , Nujol): 330(s), 316(m), 295(m). Raman (cm^{-1}): 335(m), 320(s).

[InBr₂{*o*-C₆H₄(AsMe₂)₂}]₂[InBr₄] (11). *o*-C₆H₄(AsMe₂)₂ (0.100 g, 0.35 mmol) in toluene (2 mL) was added to a suspension of InBr₃ (0.247 g, 0.70 mmol) in toluene (10 mL), and the mixture was heated and stirred at 80 °C for 3 h. It was cooled to room temperature and the white precipitate filtered off and dried in vacuo. Yield: 82%. Anal. calcd for C₁₀H₁₆As₂Br₆In₂ (995.1): C, 12.1; H, 1.6. Found: C, 12.5; H, 1.4. 1H NMR (300 MHz, CD_2Cl_2 , 295 K): 1.88 (s, [6H], CH_3), 7.7–7.8 (m, [2H], C_6H_4). Unchanged on cooling to 200 K. ^{115}In NMR ($CH_2Cl_2/CDCl_3$, 295 K): +180 (vbr). IR (cm^{-1} , Nujol): 234(s), 203(w). Raman (cm^{-1}): 239(m), 197(vs).

[InI₂{*o*-C₆H₄(AsMe₂)₂}]₂[InI₄] (12). *o*-C₆H₄(AsMe₂)₂ (0.100 g, 0.35 mmol) in toluene (2 mL) was added to a suspension of InI₃ (0.345 g, 0.70 mmol) in toluene (10 mL), and the mixture was heated and stirred at 80 °C overnight. It was cooled to room temperature and the white precipitate filtered off and dried in vacuo. Yield: 81%. Anal. calcd for C₁₀H₁₆As₂I₆In₂ (1277.2): C, 9.4; H, 1.3. Found: C, 8.8; H, 1.4. 1H NMR (300 MHz, CD_2Cl_2 , 295 K): 1.97 (s, [6H], CH_3), 7.7–7.9 (m, [2H], C_6H_4). Unchanged on cooling to 200 K. ^{115}In NMR ($CH_2Cl_2/CDCl_3$, 295 K): –450 (vbr).

[In₂Cl₆(Et₂PCH₂CH₂PET₂)₂] (13). Et₂PCH₂CH₂PET₂ (0.205 g, 1 mmol) in toluene (2 mL) was added to a suspension of InCl₃ (0.110 g, 0.50 mmol) in toluene (2 mL), and the mixture was heated and stirred at 80 °C for 2 h. It was cooled to room temperature and the white precipitate filtered off and dried in vacuo. Yield: 50%. Anal. calcd for C₂₀H₄₈Cl₆In₂P₄ (854.9): C, 28.1; H, 5.7. Found: C, 28.1; H, 5.7. 1H NMR (300 MHz, CD_2Cl_2 , 295 K): 1.14 (q, [3H], CH_3), 1.78–1.95 (m, [3H], CH_2). $^{31}P\{^1H\}$ NMR ($CH_2Cl_2/CDCl_3$, 295 K): –21.3(s). ^{115}In NMR ($CH_2Cl_2/CDCl_3$, 295 K): +450. IR (cm^{-1} , Nujol): 314(s), 284(m). Raman (cm^{-1}): 287(m), 263(s).

X-Ray Crystallography. Brief details of the crystallographic data and refinement parameters are given in Table 1. Crystals were grown from CH_2Cl_2 solutions by vapor diffusion of *n*-hexane. Data collections used a Bruker-Nonius Kappa CCD diffractometer fitted with Mo K α radiation ($\lambda = 0.71073$ Å) and either a graphite monochromator or confocal mirrors, with the crystals held at 120 K in a nitrogen gas stream. Structure solution and refinement were straightforward,^{17,18} except as noted below, with H atoms introduced into the models in calculated positions using the default C–H distance. The anion in [In₂Cl₅{*o*-C₆H₄(AsMe₂)₂}]₂[InCl₄] was disordered and was modeled as two orientations of a tetrahedral unit with a common In atom. Both of the dichloromethane solvates had disordered solvate molecules, particularly severe in [In₂Cl₆{*o*-

$C_6H_4(PMe_2)_2\}_2\cdot nCH_2Cl_2$. In both cases, C and H were not identified, and the Cl atoms were adjusted to give sensible adp values. Selected bond lengths and angles are given in Tables 2–9.

Results

Diphosphanes. The reactions of *o*-C₆H₄(PMe₂)₂ with InX₃ (X = Cl, Br, or I) in toluene solution were carried out in 2:1, 1:1, and 1:2 InX₃/diphosphane molar ratios (see Scheme 1). The reactions in a 2:1 ratio gave white complexes of composition 2InX₃/*o*-C₆H₄(PMe₂)₂, and crystals of two examples grown from CH_2Cl_2/n -hexane were found by X-ray crystallographic studies to be [InX₂{*o*-C₆H₄(PMe₂)₂}]₂[InX₄] (X = Br (2) or I (3)), containing distorted tetrahedral cations and tetrahedral anions (Figures 1 and 2, Table 2). The cations are distorted by the rigid chelate with <P–In–P ~ 84°, while the <X–In–X are much wider (X = Br, 121.85(6)° and X = I, 133.75(2)°). The In–P distances are little different between the two cations (2.552(3) Å, X = Br; 2.5575(9) Å, X = I), although rather longer *d*(In–P)'s are present in the cation [InI₂{*o*-C₆H₄(PPh₂)₂}]⁺ containing the bulkier and weaker donor aryl diphosphane (2.5862(11), 2.5635(11) Å).¹¹ The *d*(In–P) in diphosphane-bridged [(InI₃)₂(Ph₂P(CH₂)₂PPh₂)] and [(InI₃)₃(Ph₂P(CH₂)₂PPh₂)₂] are longer still (2.6523(6)–2.798(3) Å).^{9,10} The IR and Raman spectra of all three complexes (Experimental Section) are consistent with the [InX₂{*o*-C₆H₄(PMe₂)₂}]₂[InX₄] formulation, showing the characteristic features of the [InX₄][–] anions.¹⁹ The 1H and $^{31}P\{^1H\}$ NMR spectra show only a single species present in CH_2Cl_2 solution for each complex over the temperature range 295–200 K. Notably, the PMe resonances in the 1H NMR spectra are clearly defined second-order “triplets” ($^2J + ^5J = 4–6$ Hz) which compare with broad singlets in most of the other indium complexes in this study (vide infra). The $^{31}P\{^1H\}$ NMR spectra show small high-frequency coordination shifts from the free diphosphane ($\delta = -55$) with a clear trend: X = Cl, $\delta = -36.5$; X = Br, $\delta = -38.2$; X = I, $\delta = -42.2$. ^{115}In NMR spectroscopy was also used, but despite the high sensitivity and abundance of this isotope, the substantial quadrupole moment²⁰ results in fast quadrupolar relaxation and unobservably broad lines in all but near cubic environments. In practice, only the tetrahedral [InX₄][–] anions gave observable resonances, and even here the lines are broad ($w_{1/2} \sim 2000$ Hz), but these are a useful confirmation of the presence of these anions in solution.

The reaction of InX₃ (X = Cl or Br) with *o*-C₆H₄(PMe₂)₂ in a 1:1 or 1:2 molar ratio in hot toluene produced white complexes of stoichiometry InX₃/*o*-C₆H₄(PMe₂)₂, but using InI₃, the product was InI₃/1.5 *o*-C₆H₄(PMe₂)₂. The crystal structure of the bromide complex showed it to be *trans*-[InBr₂{*o*-C₆H₄(PMe₂)₂}]₂[InBr₄] (4) (Table 3, Figure 3)

(19) Tetrahedral [InX₄][–] shows one IR active stretch (ν_3 , t_2) and two Raman active stretches (ν_3 , t_2 and ν_1 , a_1). Literature values (cm^{-1}) are: X = Cl, $\nu_1 = 321$, $\nu_3 = 337$; X = Br, $\nu_1 = 197$, $\nu_3 = 239$; X = I, $\nu_1 = 139$, $\nu_3 = 185$. Data from: Nakamoto, K. *IR Spectra of Inorganic and Coordination Compounds*, 2nd ed.; Wiley: New York, 1970.

(20) ^{115}In , 95.7%, $I = 9/2$, $\Xi = 21.914$ MHz, $Q = 1.16 \times 10^{-28}$ m², $D_c = 1890$; Mason, J. *Multinuclear NMR*, Plenum: New York, 1987. ^{115}In NMR chemical shifts for the [InX₄][–] anions are (CH_2Cl_2 solution): X = Cl, +455; X = Br, +177; X = I, –569.

(17) Program for crystal structure solution: Sheldrick, G. M. *SHELXS-97*; University of Göttingen: Göttingen, Germany, 1997.

(18) Program for crystal structure refinement: Sheldrick, G. M. *SHELXL-97*; University of Göttingen: Göttingen, Germany, 1997.

Table 1. Summary of Crystallographic Data^a

	[InBr ₂ { <i>o</i> -C ₆ H ₄ (PMe ₂) ₂ }] [InBr ₄]	[InI ₂ { <i>o</i> -C ₆ H ₄ (PMe ₂) ₂ }] [InI ₄]	[InBr ₂ { <i>o</i> -C ₆ H ₄ (PMe ₂) ₂ }] [InBr ₄] · CH ₂ Cl ₂
formula	C ₁₀ H ₁₆ Br ₆ In ₂ P ₂	C ₁₀ H ₁₆ I ₆ In ₂ P ₂	C ₂₁ H ₃₄ Br ₆ Cl ₂ In ₂ P ₄
fw	907.27	1189.21	1190.36
cryst syst	monoclinic	orthorhombic	monoclinic
space group	<i>Pm</i> (no. 6)	<i>Pnma</i> (no. 62)	<i>C2/c</i> (no. 15)
<i>a</i> (Å)	7.0489(15)	16.322(3)	25.266(6)
<i>b</i> (Å)	10.496(3)	11.2518(15)	10.620(3)
<i>c</i> (Å)	7.984(2)	14.461(2)	15.089(4)
α (deg)	90	90	90
β (deg)	95.457(10)	90	113.129(10)
γ (deg)	90	90	90
<i>V</i> (Å ³)	588.0(2)	2655.7(7)	3723.1(16)
<i>Z</i>	1	4	4
<i>D</i> _{calcd} (g cm ⁻³)	2.562	2.974	2.124
μ (Mo Kα) (mm ⁻¹)	12.280	8.824	8.006
F(000)	414	2088	2248
R1 ^b [<i>I</i> > 2σ(<i>I</i>)]	0.049	0.023	0.086
wR2 [all data]	0.134	0.045	0.188
	[In ₂ Cl ₆ { <i>o</i> -C ₆ H ₄ (PMe ₂) ₂ }] · nCH ₂ Cl ₂	[In ₂ Cl ₅ { <i>o</i> -C ₆ H ₄ (PMe ₂) ₂ }] [InCl ₄]	[InI ₂ { <i>o</i> -C ₆ H ₄ (PMe ₂) ₂ }] [InI ₄ { <i>o</i> -C ₆ H ₄ (PMe ₂) ₂ }]
formula	C _{20.6} H _{33.2} Cl _{7.2} In ₂ P ₄	C ₂₀ H ₃₂ Cl ₉ In ₃ P ₄	C ₃₀ H ₄₈ I ₆ In ₂ P ₆
fw	889.63	1059.85	1585.54
cryst syst	orthorhombic	triclinic	monoclinic
space group	<i>Pbca</i> (no.61)	<i>P1</i> (no. 1)	<i>C2/c</i> (no. 15)
<i>a</i> (Å)	15.6164(15)	8.047(4)	13.8134(15)
<i>b</i> (Å)	14.3423(15)	9.393(5)	11.9283(15)
<i>c</i> (Å)	15.836(2)	12.944(7)	28.538(4)
α (deg)	90	101.94(2)	90
β (deg)	90	93.56(3)	96.006(6)
γ (deg)	90	93.30(3)	90
<i>V</i> (Å ³)	3546.9(7)	952.9(8)	4676.4(10)
<i>Z</i>	4	1	4
<i>D</i> _{calcd} (g cm ⁻³)	1.666	1.847	2.252
μ (Mo Kα) (mm ⁻¹)	2.034	2.611	5.173
F(000)	1749	512	2936
R1 ^b [<i>I</i> > 2σ(<i>I</i>)]	0.054	0.080	0.043
wR2 [all data]	0.143	0.171	0.110
	[In ₂ Cl ₆ { <i>o</i> -C ₆ H ₄ (AsMe ₂) ₂ }] · nCH ₂ Cl ₂	[In ₂ Cl ₅ { <i>o</i> -C ₆ H ₄ (AsMe ₂) ₂ }] [InCl ₄]	[InI ₂ { <i>o</i> -C ₆ H ₄ (AsMe ₂) ₂ }] [InI ₄]
formula	C _{20.5} H _{33.0} As ₄ Cl _{7.0} In ₂	C ₂₀ H ₃₂ As ₄ Cl ₉ In ₃	C ₁₀ H ₁₆ As ₂ I ₆ In ₂
fw	1056.94	1235.65	1277.11
cryst syst	orthorhombic	monoclinic	orthorhombic
space group	<i>Pbca</i> (no.61)	<i>P2/c</i> (no. 13)	<i>Pnma</i> (no. 62)
<i>a</i> (Å)	15.788(3)	8.155(2)	16.276(3)
<i>b</i> (Å)	14.612(3)	9.518(3)	11.396(2)
<i>c</i> (Å)	15.944(3)	24.595(6)	14.586(3)
α (deg)	90	90	90
β (deg)	90	94.168(10)	90
γ (deg)	90	90	90
<i>V</i> (Å ³)	3678.2(10)	1904.1(8)	2705.4(8)
<i>Z</i>	4	2	4
<i>D</i> _{calcd} (g cm ⁻³)	1.909	2.155	3.135
μ (Mo Kα) (mm ⁻¹)	5.344	5.895	10.971
F(000)	2020	1168	2232
R1 ^b [<i>I</i> > 2σ(<i>I</i>)]	0.067	0.047	0.023
wR2 [all data]	0.163	0.103	0.042

^a Temperature = 120 K; wavelength (Mo Kα) = 0.71073 Å; θ(max) = 27.5°. ^b R1 = Σ|F_o - |F_c||/Σ|F_o|. wR2 = [Σw(F_o² - F_c)²/ΣwF_o⁴]^{1/2}.

containing an octahedral cation. The cation is centrosymmetric with *d*(In–P) = 2.631(4) and 2.641(4) Å, markedly longer than in the tetrahedral cation (**2**; vide supra), and <P–In–P is also smaller at 78.75°. The *d*(In–Br) in the cation (2.6521(16) Å) is much longer than those in [InBr₂{*o*-C₆H₄(PMe₂)₂}]⁺ (**2**) (2.4563(16), 2.4737(16) Å) or in [InBr₄]⁻. The IR and Raman spectra of the bulk sample are consistent with the formulation, and the ¹H, ³¹P{¹H}, and ¹¹⁵In NMR spectra show that only this complex is present in chlorocarbon solutions.

In contrast to the bromide described above, and to [InCl₂{*o*-C₆H₄(PPh₂)₂}] [InCl₄],¹¹ the crystal structure of the

1:1 InCl₃/*o*-C₆H₄(PMe₂)₂ complex unexpectedly revealed a centrosymmetric halide-bridged dimer [In₂Cl₆{*o*-C₆H₄(PMe₂)₂}] (**5**), with six-coordinate indium centers (Table 4, Figure 4). The *d*(In–P)'s of 2.628(2) and 2.658(2) Å are longer and the <P–In–P of 77.40(5)° smaller than in the distorted tetrahedral cations discussed above, a consequence of the increased coordination number. The *d*(In–Cl)'s show a range of values: In–Cl (terminal trans P) < In–Cl (terminal trans Cl) < In–Cl (bridging trans P) < In–Cl (bridging trans Cl). The IR and Raman spectra of the solid lack the characteristic features of [InCl₄]⁻, and hence the dimer structure is present in the bulk material. However, in

Table 2. Selected Bond Lengths (Å) and Angles (deg) for $[\text{InX}_2\{o\text{-C}_6\text{H}_4(\text{PMe}_2)_2\}][\text{InX}_4]$ (X = Br or I)

(X = Br ^a)			
In1–Br1	2.4737(16)	In2–Br3	2.5012(17)
In1–Br2	2.4563(16)	In2–Br4	2.4935(18)
In1–P1	2.552(3)	In2–Br5	2.4986(13)
Br2–In1–Br1	121.85(6)	P1–In1–P1a	84.16(11)
Br1–In1–P1	108.74(6)	Br–In2–Br	105.51(7)–110.70(6)
Br2–In1–P1	113.51(7)		
(X = I ^b)			
In1–I1	2.6574(6)	In2–I3	2.7301(6)
In1–I2	2.6666(6)	In2–I4	2.6995(6)
In1–P1	2.5575(9)	In2–I5	2.7021(4)
I1–In1–I2	133.75(2)	P1–In1–P1a	83.91(4)
P1–In1–I1	109.17(2)	I–In2–I	105.84(2)–111.04(2)
P1–In1–I2	104.77(2)		

^a Symmetry operation: $a = x, 1 - y, z$. ^b Symmetry operation: $a = x, 1/2 - y, z$.

solution in CH_2Cl_2 , the complex exhibits a strong ^{115}In resonance at +442 showing the presence of $[\text{InCl}_4]^-$. At room temperature the $^{31}\text{P}\{^1\text{H}\}$ NMR spectrum is a broad resonance at $\delta = -43.6$, but upon cooling, the solution splits into resonances at $\delta = -42.8$ and -44.2 (behavior is reversible with temperature), which taken together with the ^{115}In NMR data suggests partial rearrangement into *trans*- $[\text{InCl}_2\{o\text{-C}_6\text{H}_4(\text{PMe}_2)_2\}][\text{InCl}_4]$ and probably $[\text{InCl}_3\{o\text{-C}_6\text{H}_4(\text{PMe}_2)_2\}]$ in solution (note that the $^{31}\text{P}\{^1\text{H}\}$ NMR data show that neither free $o\text{-C}_6\text{H}_4(\text{PMe}_2)_2$ nor $[\text{InCl}_2\{o\text{-C}_6\text{H}_4(\text{PMe}_2)_2\}]^+$ are formed).

A small number of crystals deposited from a solution of $[\text{InCl}_2\{o\text{-C}_6\text{H}_4(\text{PMe}_2)_2\}][\text{InCl}_4]$ in CH_2Cl_2 proved to contain a polymeric cation, $[\text{In}_2\text{Cl}_5\{o\text{-C}_6\text{H}_4(\text{PMe}_2)_2\}_2][\text{InCl}_4]_n$ (**14**). The cation (Figure 5, Table 5) shows six-coordinate indium centers, each bonded to a chelating diphosphane, one terminal and three bridging chlorines, with single and double chlorine bridges alternating along the chain. It can be considered as formally derived by abstracting a chloride ligand from $[\text{In}_2\text{Cl}_6\{o\text{-C}_6\text{H}_4(\text{PMe}_2)_2\}_2]$ (**5**) with InCl_3 (to form $[\text{InCl}_4]^-$), and maintaining six-coordination at the indium by forming single chloride bridges to give the polymer chain cation. The single bridging Cl (Cl1) bonds symmetrically to the two indium atoms with a Cl–In–Cl angle close to linear. The two In–Cl1 bonds are longer than the In–Cl (bridging *trans* Cl) of the doubly bridged unit. The corresponding bond lengths are generally slightly shorter than in $[\text{In}_2\text{Cl}_6\{o\text{-C}_6\text{H}_4(\text{PMe}_2)_2\}_2]$ (**5**; compare Table 4), reflecting the effect of cation charge.

The chemistry is different again in the InI_3 system. Reaction of InI_3 with the diphosphane in a 1:1 or 1:2 molar ratio gave a complex of composition $2\text{InI}_3/3\{o\text{-C}_6\text{H}_4(\text{PMe}_2)_2\}$. The crystal structure of this complex shows it to be *trans*- $[\text{InI}_2\{o\text{-C}_6\text{H}_4(\text{PMe}_2)_2\}][\text{InI}_4\{o\text{-C}_6\text{H}_4(\text{PMe}_2)_2\}]$ (**6**; Table 6, Figure 6). The centrosymmetric cation has $d(\text{In–P}) = 2.638(2)$ Å, not significantly different than those in *trans*- $[\text{InBr}_2\{o\text{-C}_6\text{H}_4(\text{PMe}_2)_2\}_2]^+$ (**4**; see Table 3), although longer by ~ 0.08 Å than in the four-coordinate $[\text{InI}_2\{o\text{-C}_6\text{H}_4(\text{PMe}_2)_2\}]^+$ (**3**). Similarly, $d(\text{In–I})$ in the six-coordinate cation is longer (in this case by ~ 0.25 Å) than in the distorted tetrahedral $[\text{InI}_2\{o\text{-C}_6\text{H}_4(\text{PMe}_2)_2\}]^+$ (**3**), showing that the In–I's are the dominant interactions. Comparison between

the six-coordinate anion and cation shows that the $d(\text{In–P})$ is ~ 0.05 Å longer in the former. In the anion, the $d(\text{In–I})_{\text{transI}}$ is $2.9362(5)$ Å, whereas $d(\text{In–I})_{\text{transP}}$ is $2.7923(7)$ Å.

The characterization of the octahedral anion is notable; although such species have been suggested from time to time,^{1–3} a search of the CCDB showed only one structurally authenticated example²¹— $[\text{H}_2\text{TMEDA}][\text{InCl}_4(\text{TMEDA})_2]$ (TMEDA = $\text{Me}_2\text{N}(\text{CH}_2)_2\text{NMe}_2$). In solution, the complex partially decomposes into $[\text{InI}_4]^-$, observed in the ^{115}In NMR spectrum. At 295 K, the $^{31}\text{P}\{^1\text{H}\}$ NMR spectrum is a broad resonance at $\delta = -52.7$, but upon cooling, the solution splits to show a resonance at $\delta = -46.8$ attributed to the *trans*- $[\text{InI}_2\{o\text{-C}_6\text{H}_4(\text{PMe}_2)_2\}_2]^+$ cation and a sharp feature at $\delta = -55.0$, indicating free diphosphane.

In view of the unexpected structural diversity in the indium complexes of this diphosphane, we re-examined the $\text{InX}_3/o\text{-C}_6\text{H}_4(\text{PPh}_2)_2$ systems¹¹ using $^{31}\text{P}\{^1\text{H}\}$ VTNMR and ^{115}In NMR and also examined the effect of adding excess diphosphane to the solutions. Our results are in excellent agreement with the published data, and we found no other species in the bromide or iodide systems. A solution of *trans*- $[\text{InCl}_2\{o\text{-C}_6\text{H}_4(\text{PPh}_2)_2\}][\text{InCl}_4]$ in CH_2Cl_2 exhibited a broad $^{31}\text{P}\{^1\text{H}\}$ resonance at $\delta = -26.0$ (295 K), but upon cooling the solution below 273 K this split into sharp features at $\delta = -17.4$ and -25.6 ; there was no evidence for free $o\text{-C}_6\text{H}_4(\text{PPh}_2)_2$ ($\delta = -13.0$). From a consideration of the chemical shifts of the other complexes,¹¹ we tentatively identify the two species as *trans*- $[\text{InCl}_2\{o\text{-C}_6\text{H}_4(\text{PPh}_2)_2\}_2]^+$ and $[\text{InCl}_3\{o\text{-C}_6\text{H}_4(\text{PPh}_2)_2\}]$, the absence of free diphosphane ruling out $[\text{InCl}_2\{o\text{-C}_6\text{H}_4(\text{PPh}_2)_2\}]^+$ as a possibility.

Previous studies of some p-block halide complexes of arylphosphanes and diphosphanes have shown that in chlorocarbon solutions these are slowly converted to the corresponding phosphane oxides by dry dioxygen, for example, SnX_4 or GeF_4 adducts,²² while gallium(III) complexes do not promote oxidation but are readily hydrolyzed to $[\text{PR}_3\text{H}][\text{GaX}_4]$.^{13,23,24} We find that the InX_3 complexes of $o\text{-C}_6\text{H}_4(\text{PPh}_2)_2$ show neither type of reaction. Dichloromethane solutions of $[\text{InX}_3\{o\text{-C}_6\text{H}_4(\text{PPh}_2)_2\}]$ were unchanged after three weeks exposure to dry O_2 , while upon the addition of small amounts of water, the diphosphane was displaced but without the formation of phosphonium tetrahaloindate(III).

The aliphatic backboned diphosphane, $\text{Et}_2\text{P}(\text{CH}_2)_2\text{PEt}_2$, which normally chelates to transition metals, unexpectedly behaved exclusively as a bridging ligand toward GaX_3 , forming $[\text{X}_3\text{Ga}\{\mu\text{-Et}_2\text{P}(\text{CH}_2)_2\text{PEt}_2\}\text{GaX}_3]$.¹³ However, upon reaction with InCl_3 in toluene in either a 1:2 or 1:1 $\text{InCl}_3/\text{ligand}$ molar ratio, the poorly soluble complex formulated $[\text{In}_2\text{Cl}_6\{\text{Et}_2\text{P}(\text{CH}_2)_2\text{PEt}_2\}_2]$ (**13**) was isolated. The IR and

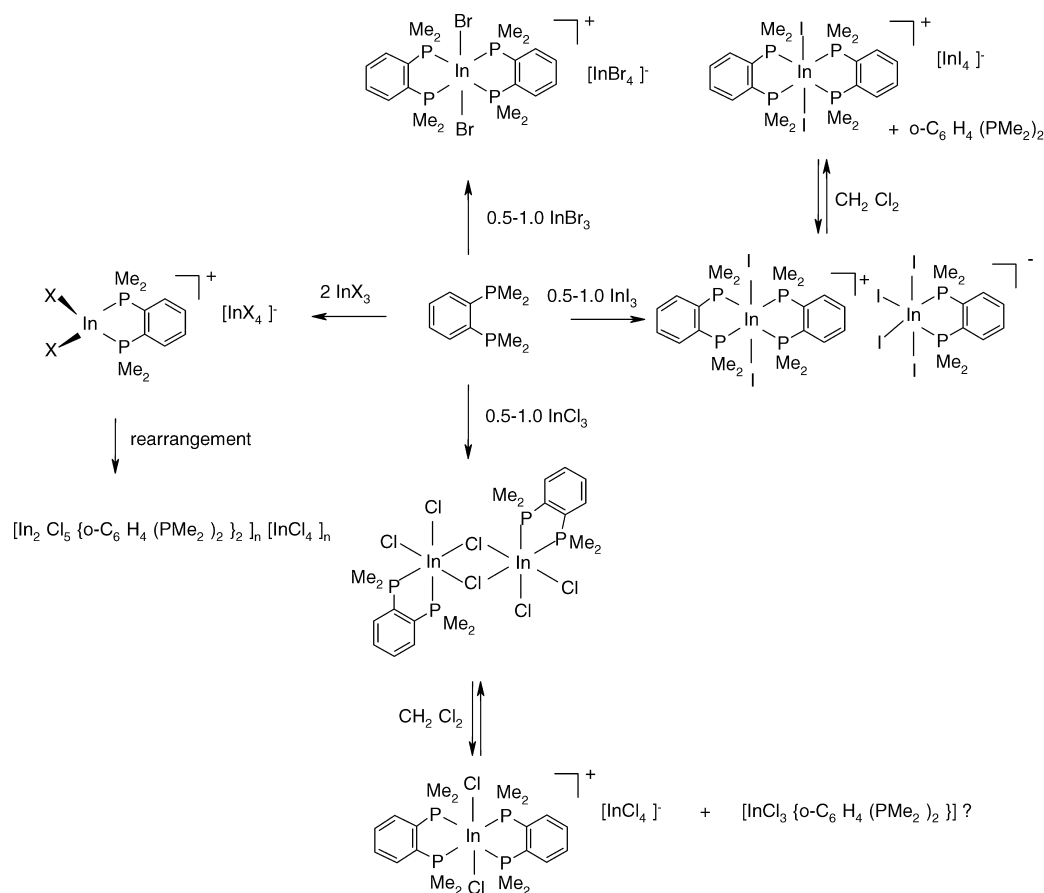
(21) Chitsaz, S.; Brehan, T.; Pauls, J.; Neumueller, B. *Z. Anorg. Allgem. Chem.* **2002**, 628, 956–964.

(22) (a) Levason, W.; Patel, R.; Reid, G. *J. Organomet. Chem.* **2003**, 688, 280–282. (b) Davis, M. F.; Levason, W.; Reid, G.; Webster, M. *Dalton Trans.* **2008**, 2261–2269. (c) Davis, M. F.; Clarke, M.; Levason, W.; Reid, G.; Webster, M. *Eur. J. Inorg. Chem.* **2006**, 2773–2782.

(23) Cheng, F.; Codgbrook, H. L.; Hector, A. L.; Levason, W.; Reid, G.; Webster, M.; Zhang, W. *Polyhedron* **2007**, 26, 4147–4155.

(24) Sigl, M.; Schier, A.; Schmidbaur, H. *Z. Naturforsch., B: Chem. Sci.* **1998**, 53, 1313–1315.

Scheme 1



Raman spectra show no evidence for $[\text{InCl}_4]^-$, although there are strong $\nu(\text{InCl})$ vibrations at 287 and 267 cm^{-1} , which are similar to those in the dimeric $[\text{In}_2\text{Cl}_6\{\text{o-C}_6\text{H}_4(\text{PMe}_2)_2\}_2]$ (**5**), and it seems likely to have a similar structure. The complex is very poorly soluble in CH_2Cl_2 , in which it gives a broad singlet $^{31}\text{P}\{^1\text{H}\}$ NMR resonance ($\delta = -21.4$) and a weak resonance at $+450$ in the ^{115}In NMR spectrum, indicating that some $[\text{InCl}_4]^-$ is present, either due to rearrangement or trace hydrolysis. Poor solubility prevented low-temperature NMR studies.

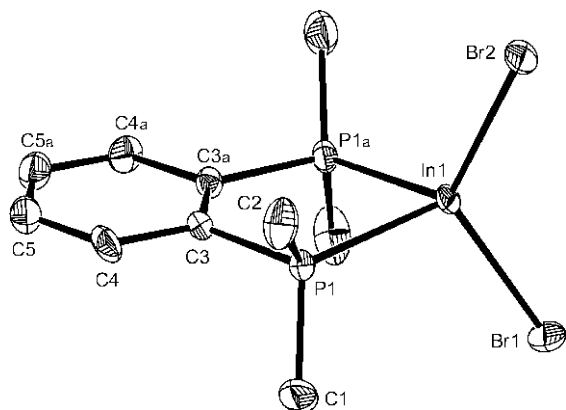


Figure 1. Crystal structure of the cation in $[\text{InBr}_2\{\text{o-C}_6\text{H}_4(\text{PMe}_2)_2\}][\text{InBr}_4]$ (**2**) showing the atom numbering scheme adopted. Ellipsoids are drawn at the 50% probability level, and H atoms are omitted for clarity. The cation has mirror plane symmetry passing through In1, Br1, and Br2. Symmetry operation: $a = x, 1 - y, z$.

Diarsanes. The previous study¹² of indium complexes of $\text{o-C}_6\text{H}_4(\text{AsMe}_2)_2$ reported 1:1 complexes with $X = \text{Cl}$ or Br and 2:3 complexes with InI_3 . These were tentatively formulated as $[\text{InX}_2\{\text{o-C}_6\text{H}_4(\text{AsMe}_2)_2\}_2][\text{InX}_4]$ and $[\text{InI}_2\{\text{o-C}_6\text{H}_4(\text{AsMe}_2)_2\}_2][\text{InI}_4\{\text{o-C}_6\text{H}_4(\text{AsMe}_2)_2\}]$, respectively, on

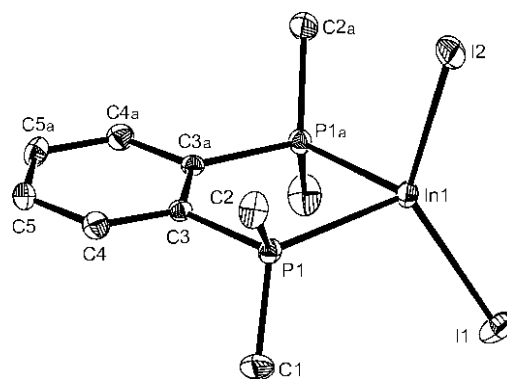


Figure 2. Crystal structure of the cation in $[\text{InI}_2\{\text{o-C}_6\text{H}_4(\text{PMe}_2)_2\}][\text{InI}_4]$ (**3**) showing the atom numbering scheme adopted. Ellipsoids are drawn at the 50% probability level, and H atoms are omitted for clarity. The cation has mirror plane symmetry passing through In1, I1, and I2. Symmetry operation: $a = x, 1/2 - y, z$.

Table 3. Selected Bond Lengths (\AA) and Angles (deg) for $[\text{InBr}_2\{\text{o-C}_6\text{H}_4(\text{PMe}_2)_2\}_2][\text{InBr}_4] \cdot \text{CH}_2\text{Cl}_2$

In1–Br1	2.6521(16)	In2–Br2	2.4996(19)
In1–P1	2.631(4)	In2–Br3	2.5116(19)
In1–P2	2.641(4)		
P1–In1–P2	78.75(12)	P2–In1–Br1	92.61(9)
P1–In1–Br1	93.97(9)	Br–In2–Br	106.8(1)–110.4(1)

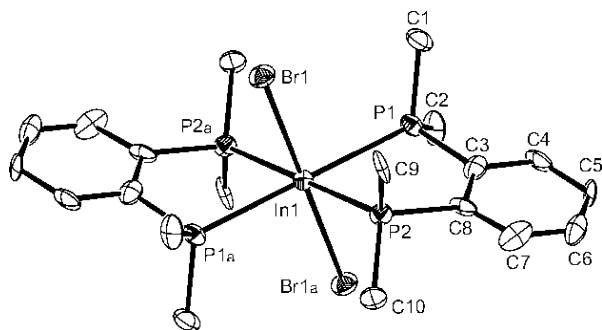


Figure 3. Crystal structure of the cation in $[\text{InBr}_2\{\text{o-C}_6\text{H}_4\text{(PMe}_2)_2\}_2][\text{InBr}_4]\cdot\text{CH}_2\text{Cl}_2$ (**4**) showing the atom numbering scheme adopted. Ellipsoids are drawn at the 50% probability level, and H atoms are omitted for clarity. The cation is centrosymmetric. Symmetry operation: $a = 1 - x, 1 - y, 1 - z$.

Table 4. Selected Bond Lengths (Å) and Angles (deg) for $[\text{In}_2\text{Cl}_6\{\text{o-C}_6\text{H}_4\text{(PMe}_2)_2\}_2]\cdot n\text{CH}_2\text{Cl}_2^a$

In1—Cl1	2.4389(15)	In1—P1	2.6278(16)
In1—Cl2	2.4736(16)	In1—P2	2.6575(15)
In1—Cl3	2.5721(14)	In1—Cl3a	2.6555(15)
Cl1—In1—Cl2	100.06(5)	P1—In1—P2	77.40(5)
Cl1—In1—Cl3	93.63(5)	Cl1—In1—P1	90.53(5)
Cl2—In1—Cl3	90.86(5)	Cl2—In1—P1	92.01(5)
Cl1—In1—Cl3a	89.64(5)	Cl3a—In1—P1	93.69(5)
Cl3—In1—Cl3a	82.70(5)	Cl2—In1—P2	84.67(5)
In1—Cl3—In1a	97.30(5)	Cl3—In1—P2a	87.05(5)
Cl3—In1—P2	98.16(5)		

^a Symmetry operation: $a = 1 - x, 1 - y, 1 - z$.

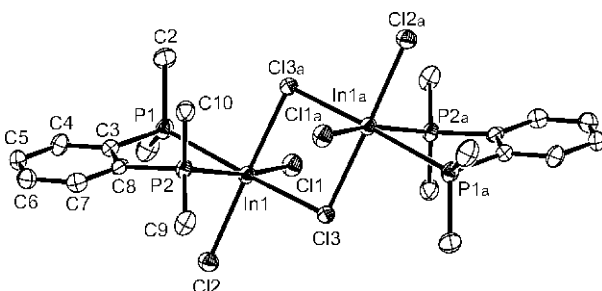


Figure 4. Crystal structure of $[\text{In}_2\text{Cl}_6\{\text{o-C}_6\text{H}_4\text{(PMe}_2)_2\}_2]\cdot n\text{CH}_2\text{Cl}_2$ (**5**) showing the atom numbering scheme adopted. Ellipsoids are drawn at the 50% probability level; H atoms are omitted for clarity, and the disordered solvate molecule has been omitted. The dimeric molecule is centrosymmetric. Symmetry operation: $a = 1 - x, 1 - y, 1 - z$.

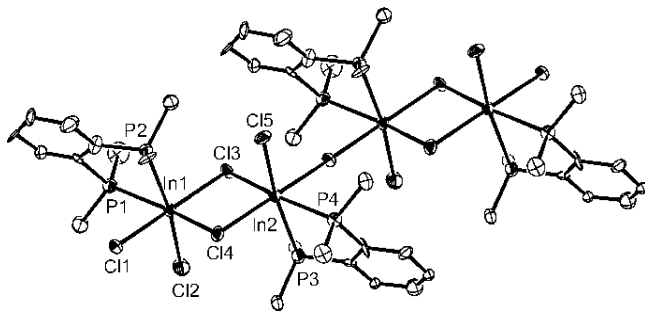


Figure 5. Crystal structure of the cation in $[\text{In}_2\text{Cl}_5\{\text{o-C}_6\text{H}_4\text{(PMe}_2)_2\}_2]_n[\text{InCl}_4]_n$ (**14**) showing the atom numbering scheme adopted. Ellipsoids are drawn at the 50% probability level, and H atoms are omitted for clarity. The cation forms a chain structure with Cl1 symmetrically bridging two In atoms.

the basis of solution conductivity and molecular weight data.¹² We find that reactions of the appropriate InX_3 with the diarsane in 1:1 and 1:2 molar ratios in toluene resulted in isolation of only a single complex from each halide

Table 5. Selected Bond Lengths (Å) and Angles (deg) for $[\text{In}_2\text{Cl}_5\{\text{o-C}_6\text{H}_4\text{(PMe}_2)_2\}_2][\text{InCl}_4]^a$

In1—Cl1	2.618(6)	In2—Cl3	2.627(5)
In1—Cl2	2.398(6)	In2—Cl4	2.536(5)
In1—Cl3	2.536(5)	In2—Cl5	2.423(5)
In1—Cl4	2.613(5)	In2—Cl1a	2.599(6)
In1—P1	2.608(6)	In2—P3	2.614(6)
In1—P2	2.612(5)	In2—P4	2.601(5)
In3—Cl6	2.374(6)	In3—Cl8	2.346(6)
In3—Cl7	2.306(7)	In3—Cl9	2.351(6)
P1—In1—P2	79.47(16)	P3—In2—P4	79.16(18)
Cl2—In1—Cl4	93.08(19)	Cl5—In2—Cl1	93.1(2)
Cl4—In1—Cl1	84.62(19)	Cl5—In2—Cl4	94.44(18)
Cl2—In1—Cl3	94.77(19)	Cl5—In2—Cl3	92.51(17)
Cl2—In1—Cl1	92.0(2)	Cl1a—In2—Cl3	84.79(18)
Cl3—In1—Cl4	86.58(16)	Cl4—In2—Cl3	86.28(16)
Cl3—In1—P1	103.91(18)	Cl4—In2—P4	104.24(18)
P1—In1—Cl2	94.35(19)	P4—In2—Cl5	94.99(17)
In1—Cl3—In2	93.40(16)	In1—Cl4—In2	93.74(18)
In2b—Cl1—In1	179.1(3)	Cl1—In3—Cl1	106.2(3)—112.2(3)

^a Symmetry operations: $a = x + 1, y, z. b = x - 1, y, z$.

Table 6. Selected Bond Lengths (Å) and Angles (deg) for $[\text{In}_2\{\text{o-C}_6\text{H}_4\text{(PMe}_2)_2\}_2][\text{In}_4\{\text{o-C}_6\text{H}_4\text{(PMe}_2)_2\}_2]^a$

In1—I1	2.9124(6)	In2—I2	2.7923(7)
In1—P1	2.6384(16)	In2—I3	2.9362(5)
In1—P2	2.6384(17)	In2—P3	2.6886(18)
P1—In1—P2	79.26(5)	I2—In2—I3b	91.452(18)
P1—In1—I1	86.31(4)	I2—In2—I3	91.698(18)
P2—In1—I1	89.62(4)	I2—In2—I2b	105.08(3)
P3—In2—I2	89.05(4)	I3—In2—I3b	174.82(3)
P3—In2—I3	85.66(4)	P3b—In2—I3	90.28(4)
P3—In2—P3b	76.94(7)		

^a Symmetry operation: $b = -x, y, 1/2 - z$.

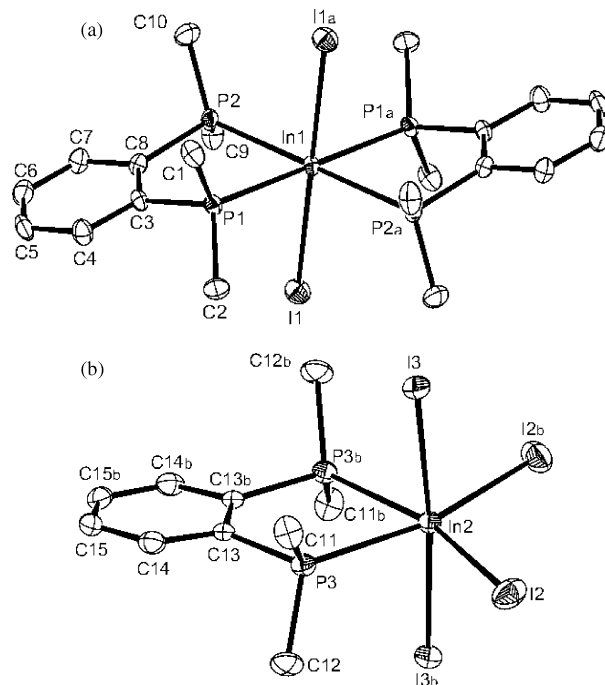


Figure 6. Crystal structure of $[\text{In}_2\{\text{o-C}_6\text{H}_4\text{(PMe}_2)_2\}_2][\text{In}_4\{\text{o-C}_6\text{H}_4\text{(PMe}_2)_2\}_2]$ (**6**) showing the atom numbering scheme adopted. Ellipsoids are drawn at the 50% probability level, and H atoms are omitted for clarity. (a) The centrosymmetric cation. Symmetry operation: $a = 1 - x, 1 - y, 1 - z$. (b) The anion showing the 2-fold symmetry. Symmetry operation: $b = -x, y, 1/2 - z$.

(see Scheme 2). However, crystals of the chloro complex, obtained from CH_2Cl_2 solution, revealed a chloride-bridged dimer structure, $[\text{In}_2\text{Cl}_6\{\text{o-C}_6\text{H}_4\text{(AsMe}_2)_2\}_2]$ (**7**). The structure (Table 7, Figure 7) is similar to $[\text{In}_2\text{Cl}_6\{\text{o-}$

Scheme 2

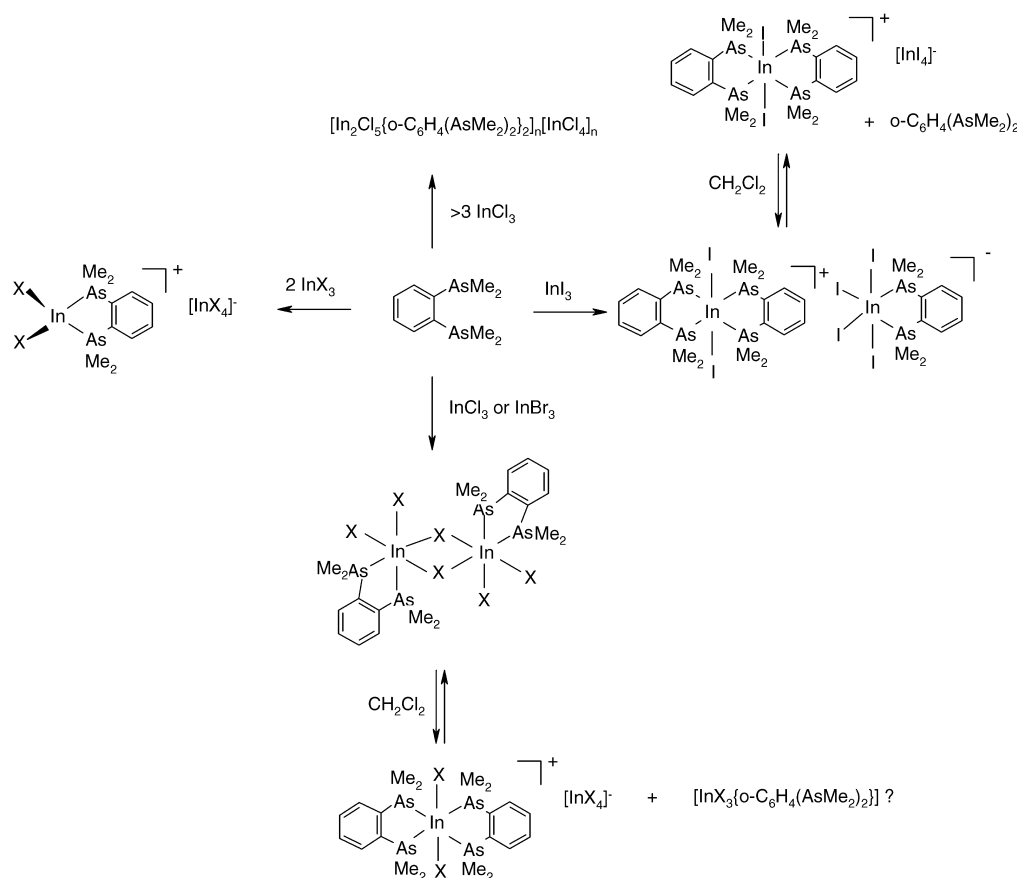


Table 7. Selected Bond Lengths (Å) and Angles (deg) for $[\text{In}_2\text{Cl}_6\{\text{o-C}_6\text{H}_4(\text{AsMe}_2)_2\}_2] \cdot n\text{CH}_2\text{Cl}_2^a$

In1–Cl1	2.423(2)	In1–Cl3	2.557(2)
In1–Cl2	2.455(2)	In1–Cl3a	2.648(2)
In1–As1	2.7134(12)	In1–As2	2.7582(12)
As1–In1–As2	77.13(3)	Cl1–In1–Cl2	101.31(9)
Cl1–In1–Cl3	94.86(8)	Cl2–In1–Cl3	91.82(8)
Cl1–In1–Cl3a	90.52(8)	Cl2–In1–Cl3a	167.71(8)
Cl3–In1–Cl3a	83.82(7)	Cl1–In1–As1	90.68(7)
Cl2–In1–As1	91.60(6)	Cl3–In1–As1	172.80(6)
Cl3a–In1–As1	91.55(5)	Cl1–In1–As2	166.92(7)
Cl2–In1–As2	83.98(6)	Cl3–In1–As2	96.93(6)
Cl3a–In1–As2	85.15(6)		

^a Symmetry operation: $a = 1 - x, 1 - y, 1 - z$.

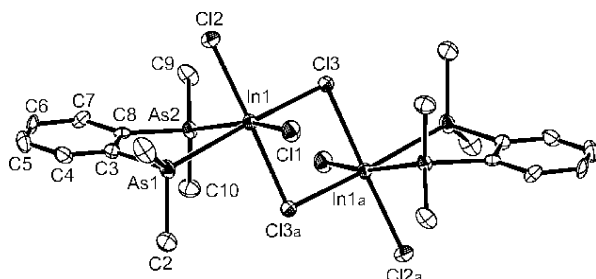


Figure 7. Crystal structure of $[\text{In}_2\text{Cl}_6\{\text{o-C}_6\text{H}_4(\text{AsMe}_2)_2\}_2] \cdot n\text{CH}_2\text{Cl}_2$ (7) showing the atom numbering scheme adopted. Ellipsoids are drawn at the 50% probability level, and the solvate and H atoms are omitted for clarity. Symmetry operation: $a = 1 - x, 1 - y, 1 - z$.

$\text{C}_6\text{H}_4(\text{PMe}_2)_2\}_2$ (5) with $d(\text{In}–\text{As}) = 2.7134(12)$ and $2.7582(12)$ Å and with $\angle\text{As}–\text{In}–\text{As} = 77.13(3)^\circ$. Some rearrangement occurs upon dissolving the diarsane complex in CH_2Cl_2 since the solution shows an ^{115}In NMR

resonance at $\delta = +451$ due to $[\text{InCl}_4]^-$, and while there is a single methyl resonance in the ^1H NMR spectrum at 295 K, upon cooling the solution, two closely spaced methyl resonances are seen, tentatively attributed to $[\text{InCl}_2\{\text{o-C}_6\text{H}_4(\text{AsMe}_2)_2\}_2]^+$ and $[\text{InCl}_3\{\text{o-C}_6\text{H}_4(\text{AsMe}_2)_2\}]$. The vibrational spectroscopic data on $[\text{In}_2\text{Br}_6\{\text{o-C}_6\text{H}_4(\text{AsMe}_2)_2\}_2]$ (8) are analogous, and this too is formulated as a halide-bridged dimer, in contrast to the ionic form found with the diphospane (vide supra), although again NMR studies identified rearrangement in solution to *trans*- $[\text{InBr}_2\{\text{o-C}_6\text{H}_4(\text{AsMe}_2)_2\}_2][\text{InBr}_4]$.

The $\text{InI}_3/\text{o-C}_6\text{H}_4(\text{AsMe}_2)_2$ system produces *trans*- $[\text{InI}_2\{\text{o-C}_6\text{H}_4(\text{AsMe}_2)_2\}_2][\text{InI}_4\{\text{o-C}_6\text{H}_4(\text{AsMe}_2)_2\}]$ (9), which is analogous to the diphospane complex (6) described above. In solution in CH_2Cl_2 , the complex rearranged, and the low-temperature ^1H NMR spectrum suggests that a mixture of *trans*- $[\text{InI}_2\{\text{o-C}_6\text{H}_4(\text{AsMe}_2)_2\}_2]^+$ and $\text{o-C}_6\text{H}_4(\text{AsMe}_2)_2$ are present. The ^{115}In NMR spectrum contains a very broad feature at -450 ppm, attributable to $[\text{InI}_4]^-$. In passing, we note that the ^{115}In NMR resonances in several of the diarsane systems are unusually broad, which probably indicates some involvement in dynamic equilibria between various indium species.

The reaction of InX_3 with $\text{o-C}_6\text{H}_4(\text{AsMe}_2)_2$ in a 2:1 molar ratio gave products with a 2:1 stoichiometry, which proved to be $[\text{InX}_2\{\text{o-C}_6\text{H}_4(\text{AsMe}_2)_2\}_2][\text{InX}_4]$ ($\text{X} = \text{Cl}$ (10), Br (11), or I (12)), confirmed by a crystal structure of $[\text{InI}_2\{\text{o-C}_6\text{H}_4(\text{AsMe}_2)_2\}_2][\text{InI}_4]$ (12) (Table 8, Figure 8) with a

Table 8. Selected Bond Lengths (Å) and Angles (deg) for $[\text{InI}_2\{o\text{-C}_6\text{H}_4(\text{AsMe}_2)_2\}][\text{InI}_4]^-$

In1–I1	2.6472(7)	In2–I3	2.6944(7)
In1–I2	2.6603(6)	In2–I4	2.7247(6)
In1–As1	2.6400(5)	In2–I5	2.7025(5)
I1–In1–I2	135.677(19)	I3–In2–I4	106.494(18)
I1–In1–As1	109.087(16)	I3–In2–I5	110.022(12)
I2–In1–As1	103.475(17)	I4–In2–I5	109.726(13)
As1–In1–As1a	83.85(2)	I5–In2–I5a	110.76(2)

^a Symmetry operation: $a = x, 1/2 - y, z$.

Table 9. Selected Bond Lengths (Å) and Angles (deg) for $[\text{In}_2\text{Cl}_5\{o\text{-C}_6\text{H}_4(\text{AsMe}_2)_2\}_2][\text{InCl}_4]^-$

In1–Cl1	2.5541(17)	In1–Cl2	2.6150(7)
In1–Cl1a	2.5977(17)	In1–Cl3	2.3859(19)
In1–As1	2.6891(11)	In1–As2	2.7039(10)
In2–Cl	2.188(4)–2.492(4)	Cl3–In1–Cl1a	95.16(6)
Cl3–In1–Cl1	96.39(6)	Cl3–In1–Cl2	91.87(5)
Cl1–In1–Cl1a	86.07(5)	Cl1a–In1–Cl2	87.21(4)
Cl1a–In1–As1	90.16(4)	Cl2–In1–As2	84.28(3)
Cl1–In1–As1	89.50(4)	Cl3–In1–As2	95.22(5)
Cl2–In1–As1	82.82(2)	As1–In1–As2	78.75(2)
Cl1–In1–As2	100.89(4)		

^a Symmetry operation: $a = -x, 2 - y, 1 - z$.

distorted tetrahedral cation. The crystal is isomorphous with the diphosphane analogue (Table 2). The white complexes show singlet ¹H NMR methyl resonances over the temperature range 295–200 K, and the ¹¹⁵In NMR spectra show very broad resonances in the regions expected for $[\text{InX}_4]^-$ anions (see Experimental Section).

A reaction of InCl_3 with $o\text{-C}_6\text{H}_4(\text{AsMe}_2)_2$ carried out with a >3:1 ratio of reagents serendipitously yielded a small number of crystals identified as $[\text{In}_2\text{Cl}_5\{o\text{-C}_6\text{H}_4(\text{AsMe}_2)_2\}_2][\text{InCl}_4]^-$ (**15**), which, although not isomorphous, has the same basic geometry as the diphosphane analogue (**14**), with a polymeric cation (Table 9, Figure 9) but with the $[\text{InCl}_4]^-$ anion disordered between two orientations. Comparison of $[\text{In}_2\text{Cl}_5\{o\text{-C}_6\text{H}_4(\text{AsMe}_2)_2\}_2]^+$ with the diphosphane analogue shows very similar In–Cl bond lengths, and In–As being greater than In–P by ca. 0.09 Å.

Conclusions

The chemistry of indium(III) halides with the three rigid *o*-phenylene chelates proves to be much more complicated (as summarized in Schemes 1 and 2) than that found for gallium(III).^{11,13} From a 2:1 $\text{InX}_3/\text{L-L}$ ratio, both $o\text{-C}_6\text{H}_4(\text{PMe}_2)_2$ and $o\text{-C}_6\text{H}_4(\text{AsMe}_2)_2$ produce distorted tetrahedral cations $[\text{InX}_2(\text{L-L})][\text{InX}_4]$ which are stable in noncoordinating solvents, and similar complexes form with the bulkier $o\text{-C}_6\text{H}_4(\text{PPh}_2)_2$ for $\text{X} = \text{Br}$ or I . At higher ligand ratios, the chemistry becomes more subtle with $[\text{In}_2\text{X}_6(\text{L-L})_2]$ present in solids for $\text{L-L} = o\text{-C}_6\text{H}_4(\text{PMe}_2)_2$, $\text{X} = \text{Cl}$, and $o\text{-C}_6\text{H}_4(\text{AsMe}_2)_2$, $\text{X} = \text{Cl}$ or Br , although these rearrange in solution to the ionic *trans*- $[\text{InX}_2(\text{L-L})_2][\text{InX}_4]$, and this form is isolated in solid *trans*- $[\text{InBr}_2\{o\text{-C}_6\text{H}_4(\text{PMe}_2)_2\}_2][\text{InBr}_4]$ and *trans*- $[\text{InCl}_2\{o\text{-C}_6\text{H}_4(\text{PPh}_2)_2\}_2][\text{InCl}_4]$. The subtleties in these systems are further illustrated by the isolation of two examples of polymeric cations $[\text{In}_2\text{Cl}_5(\text{L-L})_2][\text{InCl}_4]^-$. The indium iodides are anomalous in crystallizing as *trans*- $[\text{InI}_2(\text{L-L})_2][\text{InI}_4]$ for $\text{L-L} = o\text{-C}_6\text{H}_4(\text{PMe}_2)_2$ and $o\text{-C}_6\text{H}_4(\text{AsMe}_2)_2$. Although NMR studies show that the $[\text{InI}_4(\text{L-L})]^-$ are

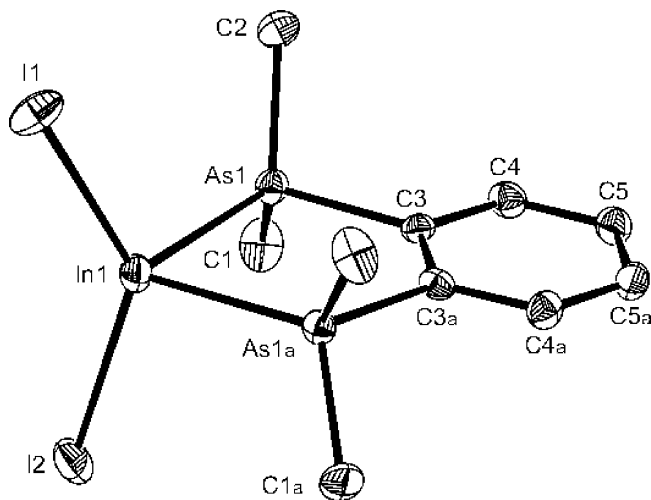


Figure 8. Crystal structure of the cation in $[\text{InI}_2\{o\text{-C}_6\text{H}_4(\text{AsMe}_2)_2\}][\text{InI}_4]^-$ (**12**) showing the atom numbering scheme adopted. Ellipsoids are drawn at the 50% probability level, and H atoms are omitted for clarity. Symmetry operation: $a = x, 1/2 - y, z$.

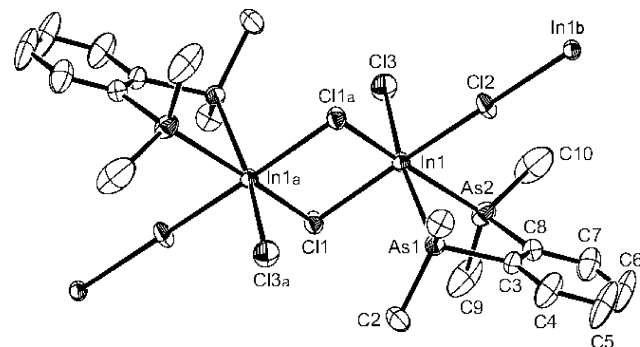


Figure 9. Crystal structure of the cation in $[\text{In}_2\text{Cl}_5\{o\text{-C}_6\text{H}_4(\text{AsMe}_2)_2\}_2][\text{InCl}_4]^-$ (**15**) showing the atom numbering scheme adopted. Ellipsoids are drawn at the 50% probability level, and H atoms are omitted for clarity. The cation forms a chain structure with alternating single and double chlorine atom bridges linking In atoms. Cl2 is on a center of symmetry. Symmetry operations: $a = -x, 2 - y, 1 - z$; $b = 1 - x, 2 - y, 1 - z$.

dissociated in solution (into L-L and $[\text{InI}_4]^-$), the formation of this complex anion in the crystals may be a consequence of the low solubility of the salt formed with the corresponding cation. It is not clear on Lewis acidity grounds why the corresponding complex anions with chloride or bromide do not form. Possibly, the energy needed to rearrange the tetrahedral InX_4 to the four-coordinate fragment of the octahedron is higher for the lighter halides, and this opposes formation of the six-coordinate anion. Although they may be present in solution, the methyl-substituted chelates do not afford solid five-coordinate adducts as found with the bulkier aryl-diphosphane in $[\text{InX}_3\{o\text{-C}_6\text{H}_4(\text{PPh}_2)_2\}]$.¹¹ The ready formation of six-coordination at indium allows the ligand $\text{Et}_2\text{P}(\text{CH}_2)_2\text{PEt}_2$ to function as a chelate compared with its unusual μ_2 mode observed in gallium(III) chemistry.

In the GaX_3 systems,¹³ usually only one complex is present in each $\text{GaX}_3/\text{L-L}$ system, and the gallium is almost always four-coordinate (distorted tetrahedral), with flexible bidentates as $[\text{X}_3\text{Ga}(\text{L-L})\text{GaX}_3]$. The rigid chelates, $o\text{-C}_6\text{H}_4(\text{AsMe}_2)_2$ and $o\text{-C}_6\text{H}_4(\text{PPh}_2)_2$, displace one X group to form cations, $[\text{GaX}_2(\text{L-L})]^+$, but only $o\text{-C}_6\text{H}_4(\text{PMe}_2)_2$ is able to

force six-coordination in *trans*-[GaX₂{*o*-C₆H₄(PMe₂)₂]₂]⁺. The spectroscopic evidence suggests that in most cases the same single form of the gallium complex is present in solution. The differences between indium and gallium are partially explained by the larger size of indium and its relatively lower Lewis acidity,^{2,3} which for indium favors higher coordination numbers and less discrimination between the various possible structures. For indium, “fine-tuning” of the structures of the In centers is possible with (P,As)₂X₂⁻, P₂X₃⁻, (P,As)₄X₂⁻, and (P,As)₂I₄-donor sets achievable, although the factors determining the isolation of a particular structure are subtle. As we noted for the gallium systems,¹³ the structural data (M–X and M–P(As) bond lengths) show

that the strongest interactions are with the halide ligands, and much weaker bonds form to P or As.

Acknowledgment. We thank RCUK (EP/C00673/1) for support, and the Daresbury Laboratory, U.K., for access to the Cambridge Structural Database.

Supporting Information Available: X-ray crystallographic data in CIF format for the compounds in Table 1. This material is available free of charge via the Internet at <http://pubs.acs.org>. Crystallographic data are also available from the Cambridge Crystallographic Data Centre with CCDC deposition numbers 689955–689963 at www.ccdc.cam.ac.uk/data_request/cif.

IC801091N